**RESEARCH**

# Fracture features of brittle coal under uniaxial and cyclic compression loads

Shikang Song[1] · Ting Ren[2] · Linming Dou[3] · Jian Sun[4] · Xiaohan Yang[5] · Lihai Tan[2,3]

## Abstract

Under the effects of complex geological and stress environments, burst hazards continue to be a major challenge for underground space utilization and deep resources exploration as its occurrence can lead to personnel causalities, equipment damage and structural collapse. Considering the stress path experienced by in-situ coal body, cyclic loading appears in quite various forms for instance shearer cutting, overlying strata breakage, hydro-fracturing and blasting, during tunnel, mining and underground space utilizing process. The stability of the underground coal body subject to periodic loading/unloading stress is extremely important for maintain the function of designed engineering structure for waste storage, safe mining, roadway development, gas recovery, carbon sequestration and so on. The mechanical properties of hard rock subject to cyclic fatigue loads has been intensively investigated by many researchers as the rock burst induced by supercritical loads has long been a safety risk and engineering problems for civil and tunneling engineering under deep overburden. More recently, the mechanical properties of coal samples under cyclic fatigue loads is investigated from the aspect of hysteresis, energy dissipation and irreversible damage as the burst hazards of brittle coal is rising in many countries. However, the crack propagation and fracture pattern of brittle coal need more research to understand the micro mechanism of burst incubation subject to cyclic fatigue loads as brittle coal can store more elastic strain energy and rapidly release the energy when its ultimate strength once reached. This research studied the internal crack status corresponding to different cyclic fatigue loading stage of brittle coal samples. The AE monitoring was applied during the uniaxial and cyclic loading process of brittle coal samples to record the crack intensity of samples at different loading stages. The damage evolution curve corresponding to loading status was then determined. The fracture pattern of coal samples determined by micro-CT scan was observed and discussed. It has been found by this paper that brittle coal of uniaxial compression tests demonstrated sudden failure caused by major splitting fracture while that of cyclic fatigue tests experienced progressive failure with mixture fracture network.

**Keywords** Fracture · Crack · Coal burst · Acoustic emission · Computed tomography

## 1 Introduction

Under the effects of complex geological and stress environments, burst hazard continue to be a major challenge for underground space utilization and deep resources exploration as its occurrence can lead to personnel causalities, equipment damage and structural collapse. Coal burst, which refers to the dynamic energy release associated by audible signal, ground vibration and displacement of fragmented coal into opening space, poses one of the highest safety and productivity risks in underground coal mines (Zhang et al. 2017; Wei et al. 2022). Thorough experimental (Peng et al. 2015; Guo et al. 2017; Feng et al. 2022) and numerical (Zhang et al. 2017; Zhao and Kaunda 2018; Tan et al. 2021) studies were conducted by researchers to

✉ Lihai Tan
 lt716@uowmail.edu.au

1   Shaanxi Zhengtong Coal Industry Co., Ltd.,
    Xianyang 713600, China

2   School of Civil, Mining and Environmental Engineering,
    University of Wollongong, Wollongong 2522, Australia

3   State Key Laboratory of Coal Resources and Safe
    Mining, China University of Mining and Technology,
    Xuzhou 221116, China

4   School of Energy and Safety Engineering, Anhui University
    of Science and Technology, Huainan 232001, China

5   School of Civil Engineering, The University of Queensland,
    Brisbane 4072, Australia

replicate the burst process of coal/rock subject to underground complex stress environment, hence to reveal the burst mechanism and develop burst mitigation methods. It has been found by Kidybinski (Kidybiński 1981) through uniaxial compression loading tests of coal samples that brittle coal tends to have more violent failure as it can storage more elastic strain energy and rapidly release the energy once the ultimate strength of coal is reached. Peng et al. (2015) conducted the conventional triaxial compression loading tests of coal samples to determine the in-situ mechanical behavior of coal under different confining pressure. The Split Hopkinson pressure bar (SHPB) system were extended to coal burst research by researchers (Li et al. 2016; Tan et al. 2020) to study the influence of extreme dynamic disturbance and coupled static-dynamic loads on the energy dissipation and burst behavior of coal.

Considering the stress path experienced by in-situ coal body, cyclic loading appears in quite various forms for instance shearer cutting, overlying strata breakage, hydro-fracturing and blasting, during tunnel, mining and underground space utilizing process (Zhang et al. 2020). Hence, key underground structures such as pillars, longwall panels and sidewalls were continuously subject to periodic loading/unloading stress. These structures, which are designed for coal extraction, gas recovery, waste storage and underground facilities, need to be stable and functional for an extended engineering life under the effect of these cyclic loads. The mechanical properties of hard rock subject to cyclic fatigue loads has been intensively investigated by many researchers (Li et al. 2019a; Wang et al. 2020; Zheng et al. 2020) as the rock burst induced by supercritical loads has long been a safety risk and engineering problems for civil and tunnelling engineering under deep overburden. More recently, the mechanical properties of coal samples under cyclic fatigue loads is investigated from the aspect of hysteresis (Zhang et al. 2020), energy dissipation (Li et al. 2019b) and irreversible damage (Fan and Liu 2019) as the burst hazards of brittle coal is rising in many countries (Frith et al. 2020; Christopher 2021). However, the crack propagation and fracture pattern of brittle coal need more research to understand the micro mechanism of burst incubation subject to cyclic fatigue loads as brittle coal can store more elastic strain energy and rapidly release the energy when its ultimate strength once reached (Yang et al. 2020).

This research aims to study the internal crack status corresponding to different cyclic fatigue loading stage of brittle coal samples. The acoustic emission (AE) monitoring was applied during the uniaxial and cyclic loading process of brittle coal samples to record the crack intensity of samples at different loading stages. The damage evolution curve corresponding to loading status was then determined according to AE information and damage mechanics. The fracture pattern of coal samples determined by Computed Tomography (CT) scan was observed and discussed.

## 2 Experiments

### 2.1 Sample preparation

The coal blocks were taken from underground longwall face and then processed into standard samples as required by International Society of Rock Mechanics (ISRM) by coring, cutting and polishing. Coring positions of coal blocks were marked on the flat surface according to the shape and bedding orientation of coal blocks. To avoid the influence of bedding angle, the coring direction remain perpendicular to the bedding direction. Coal samples were well wrapped by poly-film to keep natural status as shown in Fig. 1. Eight cylindrical samples were randomly divided into two groups for different testing purposes. Sample A1 to A4 were for uniaxial compression tests while sample A5 to A8 were for cyclic fatigue tests. All coal samples used for uniaxial compression and cyclic fatigue loading tests are from the No. 4 coal seam in Binchang coal field, Shaanxi Province, China. Exploration of the No. 4 coal seam is facing complex geo-stress environments leaded by over 800 m overburden, 7 MPa dynamic water pressure in the roof aquifer and non-uniform horizontal stress distribution. Besides, No. 4 coal seam consists of non-coking coal with high ultimate strength, which has an extremely strong burst propensity. The contents of coal revealed by industrial analysis are listed in Table 1. Since the commencement of roadways development and mining operations, massive seismic events and burst accidents have been documented by the local stress and seismicity monitoring system in the mining region.



**Fig. 1** Coal samples for uniaxial compression and cyclic fatigue loading

**Table 1** Industrial analysis of the No. 4 coal seam

| Moisture $M_{ad}$ (%) | Ash $A_{ad}$ (%) | Volatile $V_{ad}$ (%) | Sulphur (%) | Phosphorus (%) | Fixed carbon $FC_{ad}$ (%) |
|---|---|---|---|---|---|
| 1.74 | 11.23 | 32.08 | 0.63 | 0.015 | 59.86 |

## 2.2 Experimental systems and methods

The mechanical tests of all coal samples were conducted by the Rock Universal Testing Laboratory at University of Wollongong. The Instron 8033 hydro-served testing system was used to apply uniaxial compression and cyclic fatigue loads on coal samples. The linear variable differential transformer (LVDT) mounted on the upper loading plate was connected to the controlling system to update and record the real-time load vs axial displacement data for the plotting of stress vs strain figure. The loading and unloading rate for uniaxial and cyclic fatigue load were 0.5 mm/min. The Express-8 AE monitoring system was adopted to continuously log the acoustic events/micro failure inside the coal samples during the whole loading process. The sensors with a good frequency response and sensitivity were attached to the surface of the cylinder coal sample. The sampling frequency of AE system was 1 MHz and the pre-amplification was set as 45 dB. The collected data for each AE events including amplitude, frequency, time and energy. Figure 2 shows the testing devices and AE monitoring system for the uniaxial

and cyclic compression tests. For uniaxial compression tests, coal samples were uniaxially compressed till post-failure. For cyclic fatigue tests, the first unloading point was 20 kN (10.2 MPa) for all samples, which is beyond 75% of the average strength determined by uniaxial compression tests. Then the unloading point was gradually increased with an interval of 2–4 kN (1–2 MPa) for each cyclic loading cycle, which depends on the loading behavior of previous loading cycle.

## 3 Test results

### 3.1 Stress–strain curves

Based on the test data recorded by LVDT, the stress versus strain curves of all uniaxial compression and cyclic fatigue tests are plotted in Figs. 3a and b, respectively. It can be seen from the uniaxial compression tests that the coal seam is of high burst propensity. The average uniaxial compression strength is over 14 MPa, which is classified as high burst liability coal according to the Chinese Burst Liability Classification Standard (Qi et al. 2011). Besides, the post peak curves of sample A02 and A04 demonstrate a significantly stress drop corresponding to the sudden and brittle failure of samples. Sample A01 and A03 also experienced sudden stress drop after peak period. It has been revealed by previous research that the sudden failure generally indicates the catastrophic energy releasing behavior of coal samples (Singh 1988). Considering the high mining depth of the coal
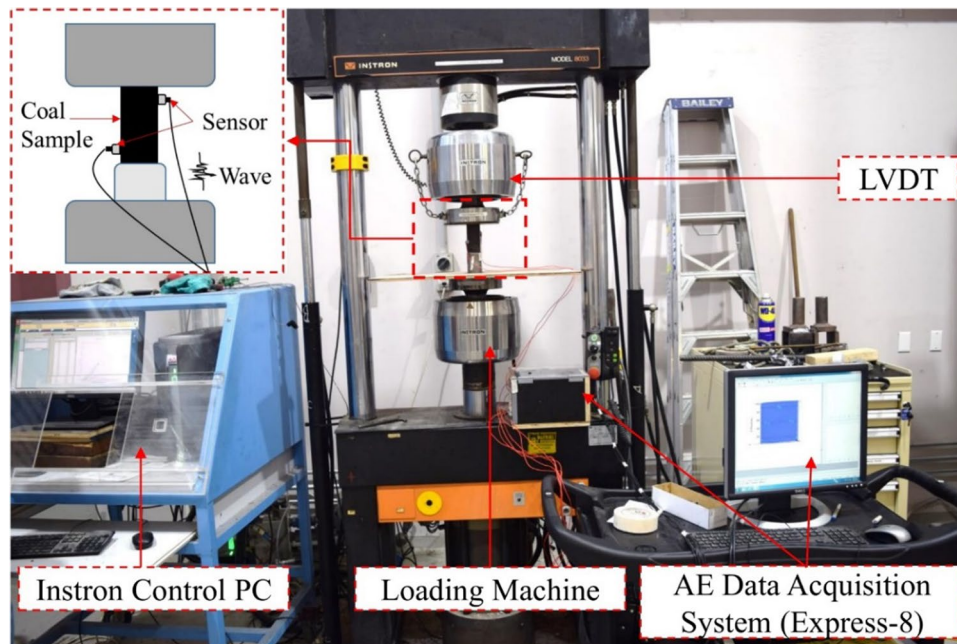


**Fig. 2** Set-up of loading machine and AE system
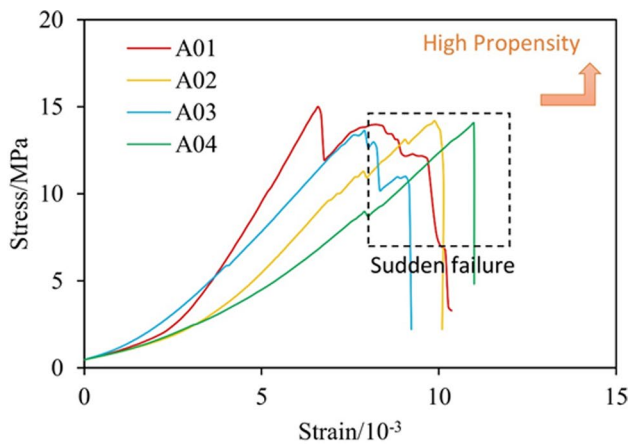
a. Stress-strain curves of uniaxial compression tests
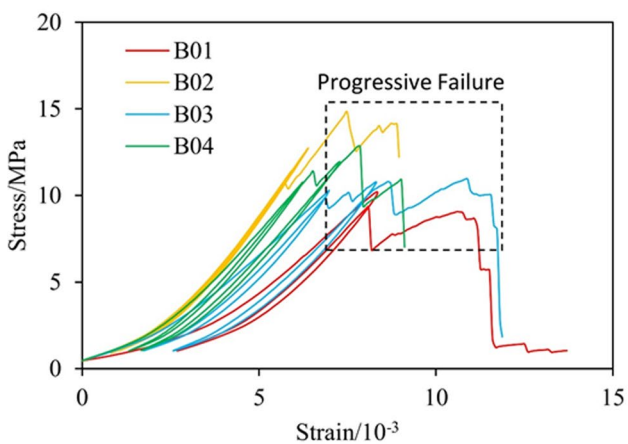

b. Stress-strain curves of cyclic fatigue tests

**Fig. 3** Stress–strain curves for all samples

**Table 2** FLC and failure load of cyclic fatigue tests (Unit: kN)

| Sample No. | FLC1 | FLC2 | FLC3 | Failure |
|---|---|---|---|---|
| B01 | 20 | Nil | Nil | 20 |
| B02 | 20 | 22 | 25 | 29 |
| B03 | 20 | 22 | Nil | 22 |
| B04 | 20 | 24 | Nil | 25 |

seam, the surrounding coal body can release massive elastic energy once the open space is excavated, which can cause potential burst hazards during the failure process of coal body.

Table 2 shows the maximum load of each fatigue loading cycle (FLC) and failure load of each sample. Different with stress path of uniaxial compression tests, all the coal samples show a progressive failure process after the ultimate strength point. Although the stress drop is as sudden as uniaxial compression, each drop magnitude is much lower than uniaxial compression tests. The average strength of cyclic fatigue

test samples is 12 MPa, which is 2 MPa lower than uniaxial compression tests. Sample B01 only experienced one FLC and then start failure process at the same level with unloading point. Sample B02 last three FLCs and then enter progressive failure stage. After two FLCs loading, sample B03 and 04 start failure process at the same level with unloading point of previous FLC. It can also be seen from the unloading path that most of energy input from loading machine will be stored as the difference between loading path and unloading path is small, which means elastic strain energy in coal samples.

The gentler failure and lower strength of coal samples subject to cyclic fatigue load could be related to the stable fracture propagation during the FLC loading process. It has been widely accepted that, as shown in Fig. 4, the typical pre-peak stress–strain curve can be classified into four phases based on the volumetric strain, i.e., Stage I crack closure, Stage II elastic deformation, Stage III stable crack development, Stage IV unstable crack development (Ranjith et al. 2010; Yao et al. 2019). The transition point between Stage III and IV is $\sigma_{cd}$, which is around 80% of strength of the sample. For the first FLC of cyclic fatigue test, the maximum load is around 75% of the average strength. That is, coal sample only experienced stage I, II and III, which allows the stable development of micro cracks inside the coal sample. The internal cracks will propagate and coalesce to form fracture surface at the post-peak stage, which makes the sample have a progressive failure process. However, the average strength of cyclic fatigue loading group is only 2 MPa lower than uniaxial compressive loading group as the damage in stage III is reversible once the load reduced.

The observed gentle failure of cyclic fatigue loading tests can support the effectiveness of application of fracturing in burst controlling as well. Fracturing of coal body has long been taken as an effective method to mitigate the burst risk (Huang et al. 2014). The facture network will be formed by hydraulic injection or de-stress blasting. But the fracture network will be closed again due to complex and high geostress environment. Based on the above analysis, the fractured coal body will have a gentler failure pattern compared with the intact coal body as the cracks have been artificially formed, but the bearing capacity of the coal body will not be obviously reduced due to the confining stress.

## 3.2 Crack propagation

AE, which is a non-destructive monitoring method of rock/coal failure, can provide a continuous and real-time record of sub-audible voice associated with crack initiation and propagation. The logged AE information of coal can include counts, amplitude, frequency, and duration etc. Because of the differences on the mode of the crack, the recorded AE parameters for each crack, as shown in Fig. 5,
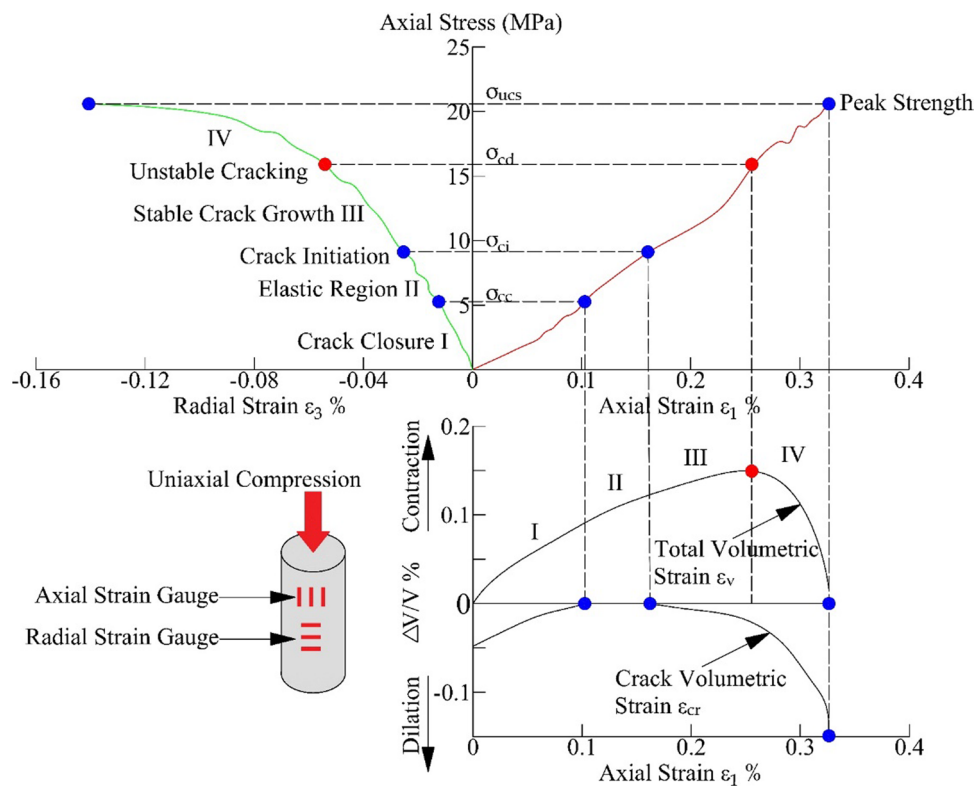
**Fig. 4** Typical stress–strain curve and fracture stages of coal sample subject to uniaxial compression load (Tan et al. 2020)
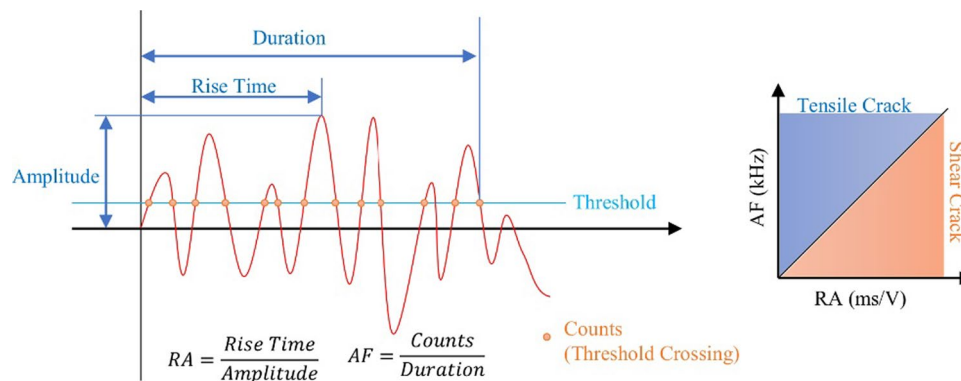


**Fig. 5** Schematic diagram of AE parameters and crack classification modified from (Aldahdooh and Bunnori 2013)

will be different, which contains the information to identify the crack types and intensity. AE counts is positively linked to the crack intensity inside coal samples (Kahirdeh et al. 2016; Zhang et al. 2021a). AF (average frequency acquired by counts divided by duration) and RA (rise time divided by amplitude) are the crucial parameters to classify the crack mode. The used Express-8 AE monitoring system in this study can automatically transform the captured waveform information by sensors into the parameter values.

To indicate the crack intensity associated with the different loading stage, the AE counts of uniaxial compression and cyclic fatigue tests are plotted in Figs. 6 and 7, respectively. In Fig. 6, at the beginning of the loading curve, no AE was recorded as the sample is in stage I and II with very limited crack activities inside the coal sample. Then the AE activity remain in low but stable level with the increase of load, which is corresponding to stage III in Fig. 4. Besides, the AE intensity is positively related to the stress drop level.

The AE counts of cyclic fatigue tests have the same feature with uniaxial compression tests. At the FLCs loading stage, the AE counts remain low and stable compared with the peak point. It should be noted that the AE counts is
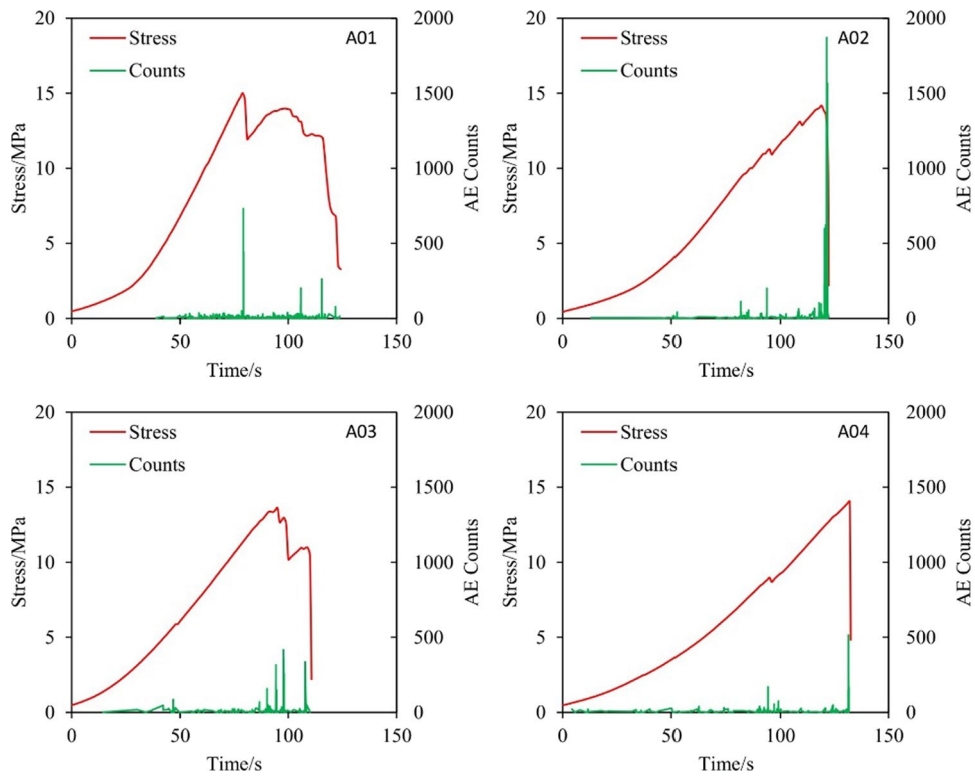
**Fig. 6** AE Counts at different loading stage of uniaxial compression tests
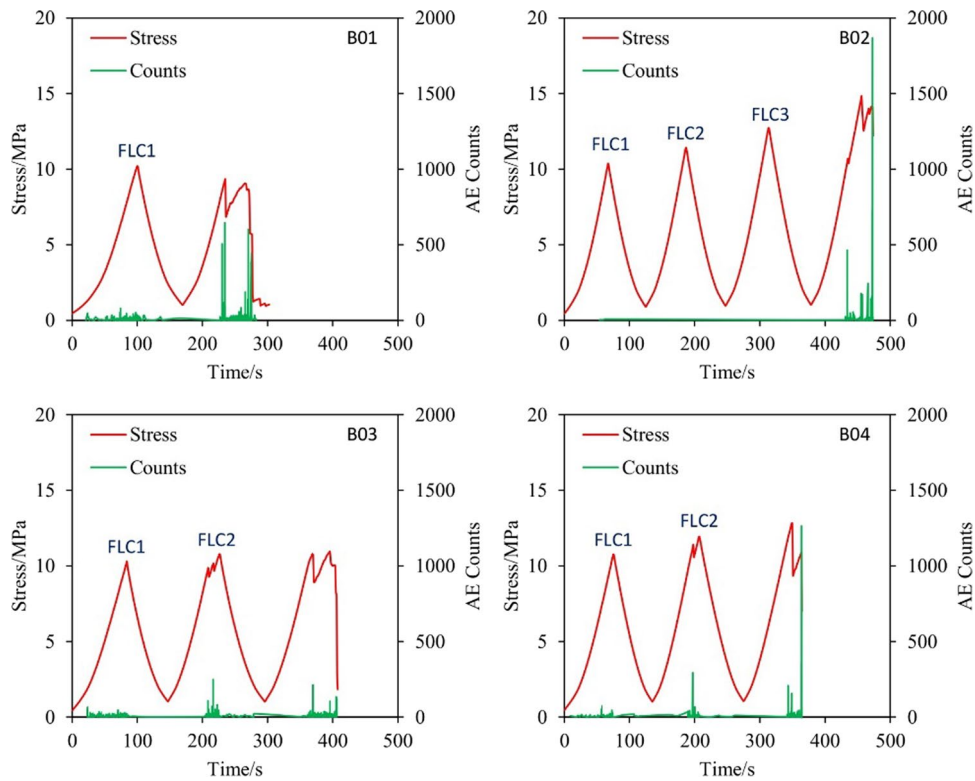


**Fig. 7** AE Counts at different loading stage of cyclic fatigue tests
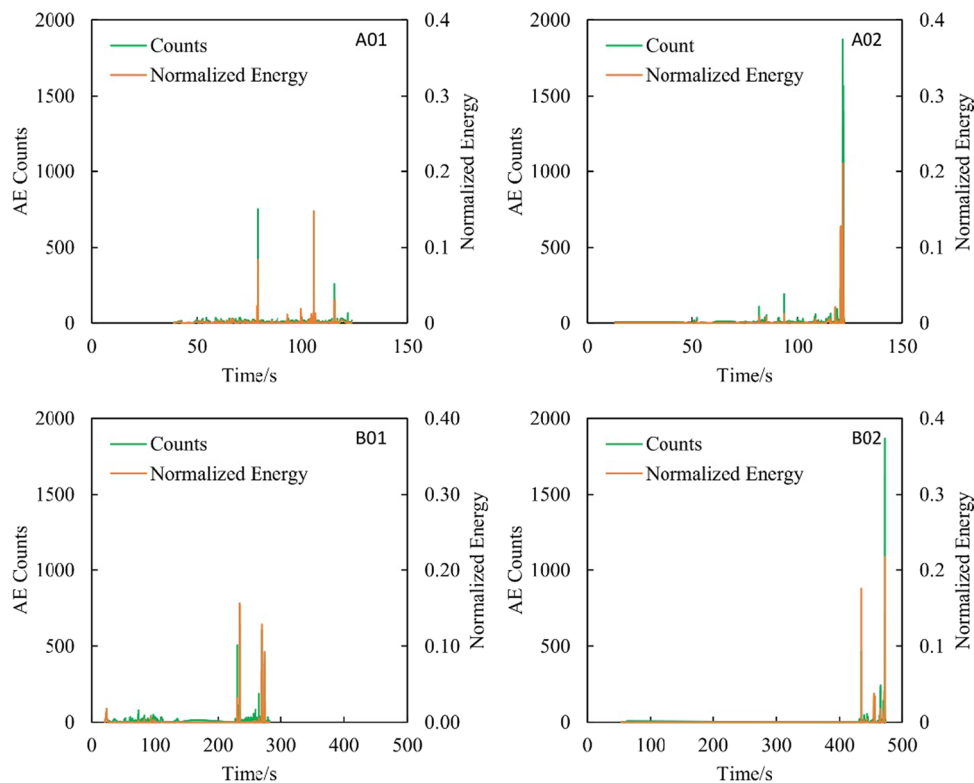
**Fig. 8** AE energy associated with cracks

only a qualitative parameter to indicate the crack intensity of one sample at different stage in this paper rather than a quantitative parameter to compare between different samples.

Beside the AE counts, the energy release associated with sample fractures is recorded as well. The energy changing trend is correlated to AE counts. In this paper, the normalized energy (energy release at certain time divided by the total AE energy) is presented, which enable the comparison between different samples. As shown in Fig. 8, the trend of energy change is same with AE counts. Besides, the energy peak is not necessarily at the same time with AE counts as demonstrated by sample A01 and B01, which should be caused by the energy level difference between micro crack and major crack.

From RA and AF parameters, cracks can be classified into tensile and shear cracks as illustrated in Fig. 5. The most widely used classification method is based on JCMS-III B5706 for concrete, which set the proportion of RA and AF values to 1:80 (Aldahdooh and Bunnori 2013; Prem and Murthy 2017). However, this proportion for coal has been studied in limited research. Hence, the 1:80 proportion is only set as reference to qualitatively describe the crack

type without a calculated percentage to quantitatively indicate each crack type. Figure 9 indicates the AF-RS analysis result of uniaxial compression tests before and after peak stress. The red dotted line is the reference line with 1:80 proportion. It can be seen from the comparison that most of the cracks are tensile at the loading stage, but more shear cracks appears while the sample enter failure stage. The tensile cracks are crack initiation at the weak points inside the coal sample under compression load (Janeiro and Einstein 2010). With the crack coalescence, the shear crack connected by the tips of the tensile crack are formed and slipped (Liu et al. 2015), which lead to stress drop or failure of the coal sample.

The RA-AF analysis results of cyclic fatigue tests are plotted in Fig. 10. Different with Fig. 9, the comparation is between FLC loading stage and failure process. For the FLC stage, most of cracks for all samples are tensile crack (over 80%). Although B02 and B03 is not obvious due to several shear failures on the *x*-axis. The crack feature of failure stage is mixture of tensile and shear crack. Besides, the coordinate of cracks in cyclic fatigue tests is closer to origin compared with uniaxial compression tests. The above AE analysis verified the crack analysis based on stress–strain curves. At the
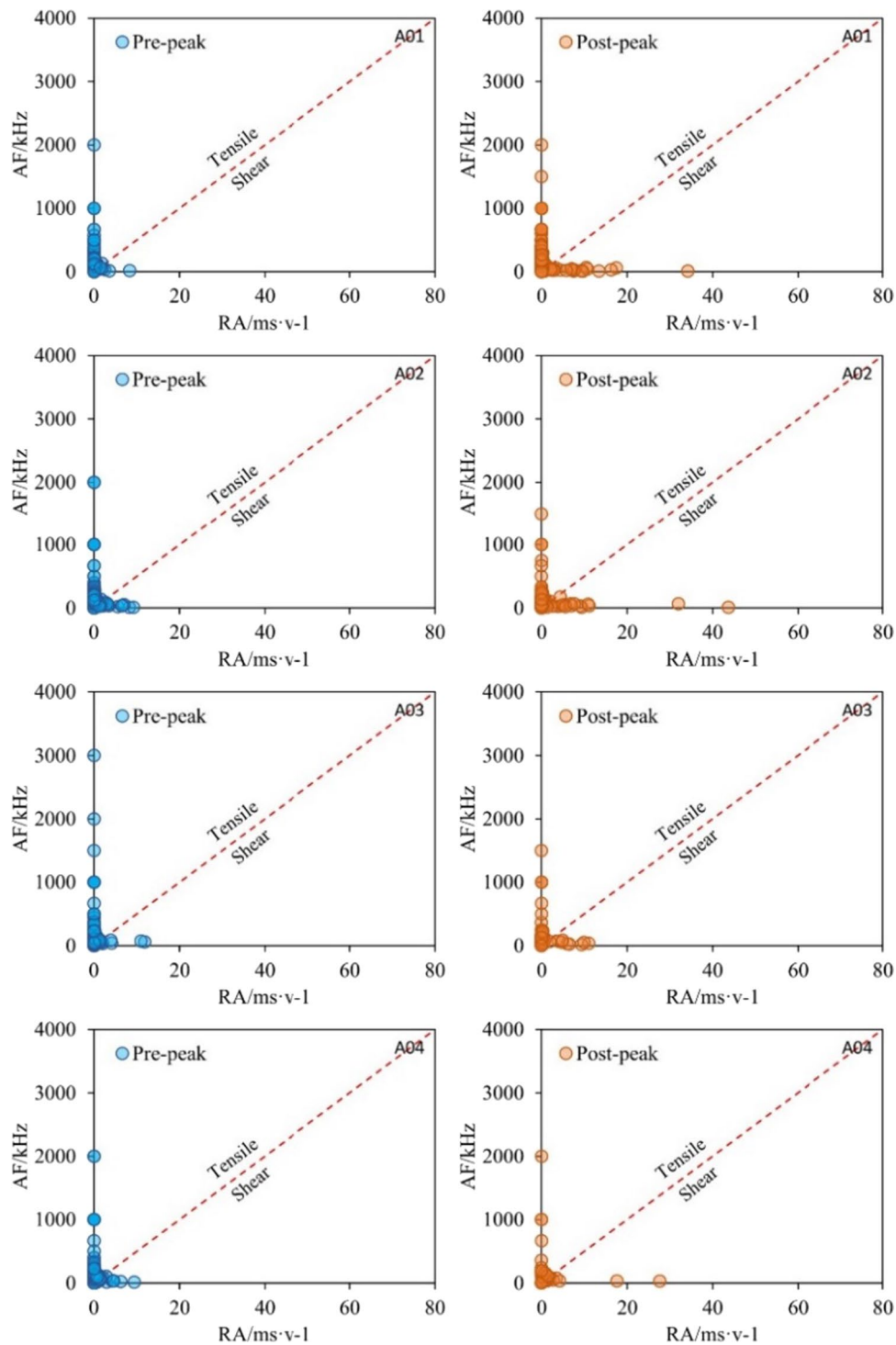
**Fig. 9** RA-AF analysis of uniaxial compression tests before and after peak stress

FLC stage, the crack activities inside the coal sample are stable as most of the cracks are tensile type. The sample will progressively fail with gentler shear failure as the shear cracks are centralized on origin.

## 3.3 Damage evolution

It has been revealed in previous research that the damage process of coal conforms to the Weibull distribution (Xie 1990),
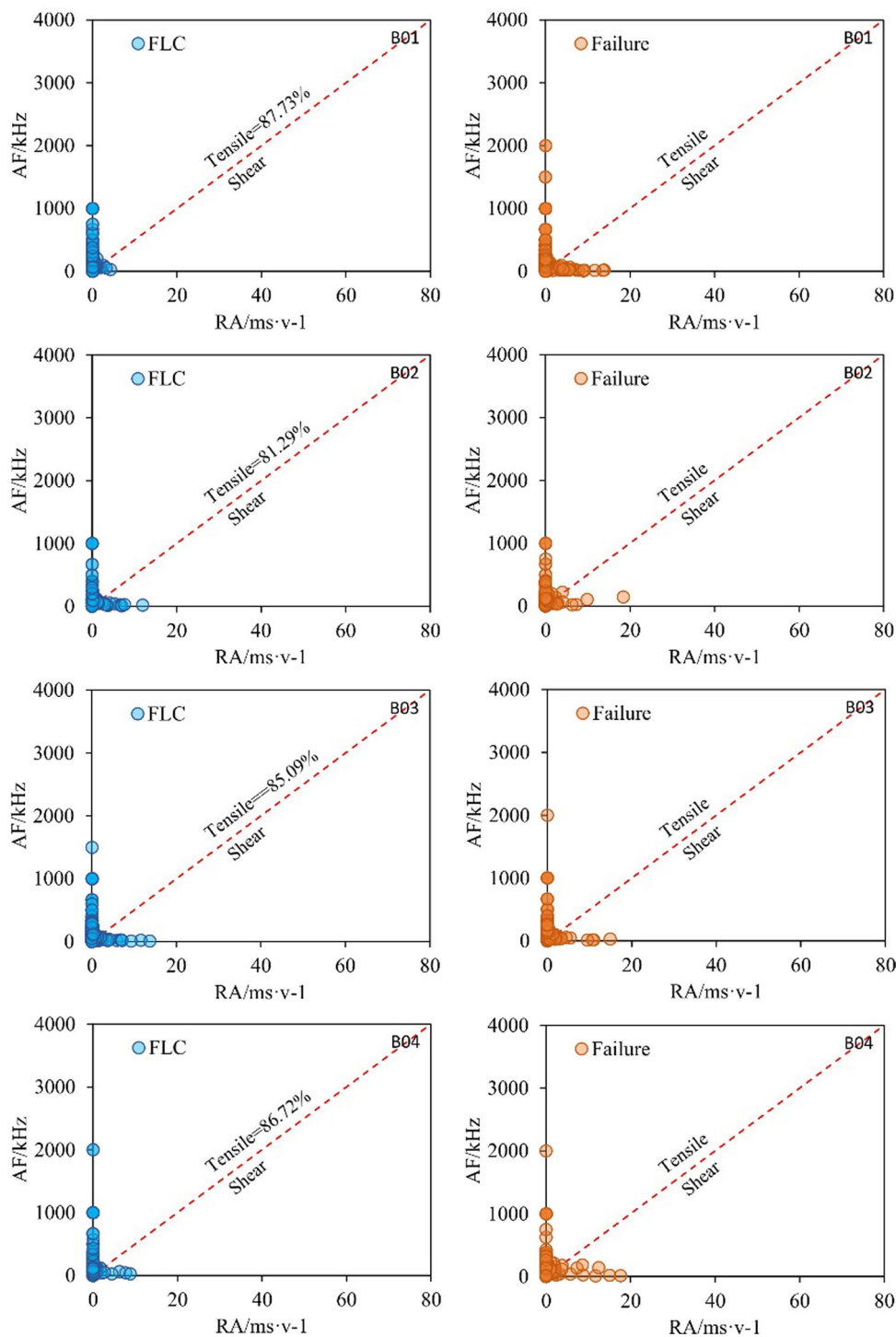
**Fig. 10** RA-AF analysis of cyclic fatigue tests before and after peak stress

and the probability density function (PDF) can be written as:

$$f(\varepsilon) = \frac{k}{\gamma} \left(\frac{\varepsilon}{\gamma}\right)^{k-1} \exp\left[-\left(\frac{\varepsilon}{\gamma}\right)^k\right] \qquad (1)$$

where $\varepsilon$ is coal strain, $k$ and $\gamma$ represent the shape parameter and scale parameter of Weibull distribution, respectively.

Then the damage factor, which is the parameter to reflect the internal damage degree of coal samples, can be acquired by:

$$\frac{\mathrm{d}D}{\mathrm{d}\varepsilon} = f(\varepsilon) \qquad (3)$$

where $D$ is damage factor which ranges from 0 (No damage) to 1 (totally damaged).

The damage factor calculation process based on AE monitoring has been introduced by previous research (Zhang et al. 2021b). The accumulative AE count $C(t)$ at any time $t$ can be expressed by:

$$C(t) = C_{total} \int_0^{\varepsilon} f(\varepsilon) dx \tag{3}$$

where $C_{total}$ is AE counts accumulated when the coal is destroyed.

Then the damage factor of coal at any time can be acquired by the record of AE count:

$$D = \frac{C(t)}{C_{total}} \tag{4}$$

For the uniaxial compression tests, the damage factor constantly increase under the compression load and the brittle failure pattern can be seen from the stress–strain curve and AE counts. The damage factor of coal samples subject to cyclic fatigue load rapidly increase at the failure stage, which indicate the samples failure is still brittle at the final stage. But during the FLCs loading stage, all samples exclude B02 have a progressive increase of damage factor. Although the damage factor remains low during this stage, this process is identical with the progressive failure observed from Fig. 3a.

# 4 Fracture pattern determined by CT

## 4.1 Scan and reconstruction

Section 3 introduced the crack features and failure pattern of coal samples subject to uniaxial compression and cyclic
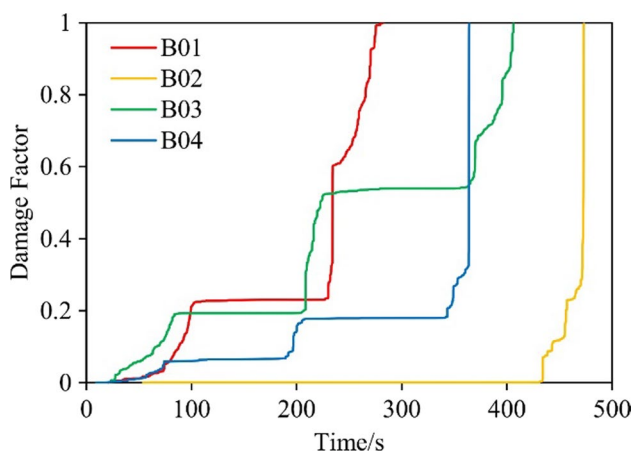


**Fig. 11** Damage evolution of coal samples subject to cyclic fatigue load

fatigue loading through stress–strain, AE, and damage data. These data are indirect demonstration of the crack and failure process of coal samples. To get a more direct observation of internal crack and fracture, a Skyscan1275 X-ray microcomputed tomography (Micro-CT) scanner is used to visualize the failed coal. The tested sample is firstly placed in the specifically designed seat to hold the sample for rotation during the 360° scan process. The scan resolution is set to high, and each pixel is set to 30 μm. The selected power of X-ray source is 100 kV and 100 μA. The scan interval is 0.2 degree, which means the samples will be clock-wisely rotated 0.2 degree for the next scan position once the previous step finished. Approximately 1800 CT images are produced for each sample. The work principle of CT scanner has been detailed introduced in literature (Zhao et al. 2021).

Once the scanning is finished, all the obtained images are used to reconstruct the 3D visualization of the sample by reconstruction software. Through optimizing the reconstruction setting such as ring reduction, smoothing etc., the reconstructed cross-sectional images are outputted (Fig. 11).

## 4.2 Results and discussion

Due to the brittle and sudden failure, the coal sample generally has obvious particle ejection behavior and only some of the sample remain considerably "intact" for CT scan. The selected typical sample for CT scanning of uniaxial compression test and cyclic fatigue test are A04 and B04, respectively (Fig. 12).

The mapped internal fractures of sample A01 are shown in Fig. 13. Two main splitting fractures (white line on the figure) through both ends can be clearly seen from the $X$–$Y$ and $X$–$Z$ segmented section view of the scanned results. The scanned image can verify the observations in Sect. 3 that the coal samples subject to uniaxial compression load experienced brittle and violent splitting failure behavior with the mixture of shear and tensile cracks. The internal fracture pattern is identical with the crack analysis based on AE data. All these fractures are associated with the instantaneous release of energy at failure point (Bieniawski et al. 1969), which could be a pressure burst or coal burst in a coal sample scale.

For the sample under cyclic fatigue load, the scanned internal structure shows an obviously different fracture network compared with sample A04 as shown in Fig. 14. The coal sample B04 is more fractured compared with the sample A04. There are two main shear fractures associated with numerous micro-cracks inside the coal sample. However, these cracks are not through the sample. The length of the cracks is much shorter than that of sample A04, which can
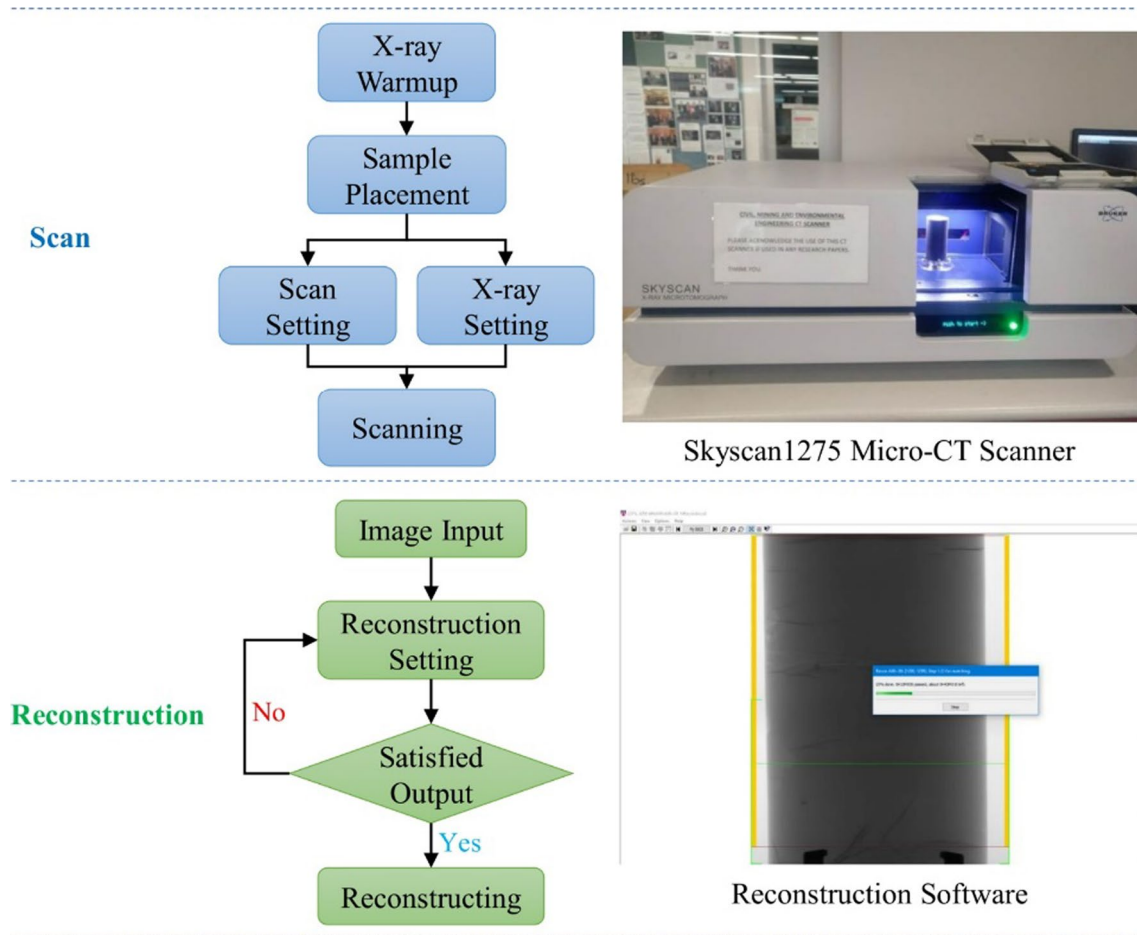
**Fig. 12** Scan and reconstruction of failed coal samples

indicate a gentler failure pattern. It has been concluded in Sect. 3 that the coal samples subject to cyclic fatigue load will develop more cracks, which can be verified by this CT observation.

## 5 Conclusions

The stability of the underground coal body subject to periodic loading/unloading stress is extremely important for maintaining the function of designed structure. This failure behavior of coal sample subject to cyclic fatigue load is compared with that of conventional uniaxial compression load in terms of stress–strain curves crack propagation, damage evolution and fracture pattern based on the AE monitoring and CT scan. The following main conclusions can be drawn based on this study:

(1) Coal samples subject to cyclic fatigue load have gentler failure and lower strength than that of uniaxial compression load, which could be related to the stable fracture propagation during the FLC loading process. The effectiveness of fracturing for burst control can also be supported by this finding as well.

(2) The AE counts of coal sample in cyclic fatigue tests indicate a stable crack initiation and accumulation process during the FLC loading stage. For the FLC stage, most of cracks are tensile crack. The crack feature of failure stage is mixture of tensile and shear crack. The sample under cyclic fatigue load will progressively fail with gentler shear failure as the shear cracks are centralized on origin.

(3) For the uniaxial compression tests, the damage factor constantly increase under the compression load and the brittle failure pattern can be seen from the stress–strain curve and AE counts. But during the FLC loading stage, all samples exclude B02 have a progressive increase of damage factor.

(4) The mapped internal cracks by CT scan indicate that the coal sample subject to uniaxial compression load experienced brittle and violent splitting failure behav-

X-Z section view with Y=25 mm

X-Y section view with Z=55 mm

Failure pattern: axial splitting with cracking through both ends
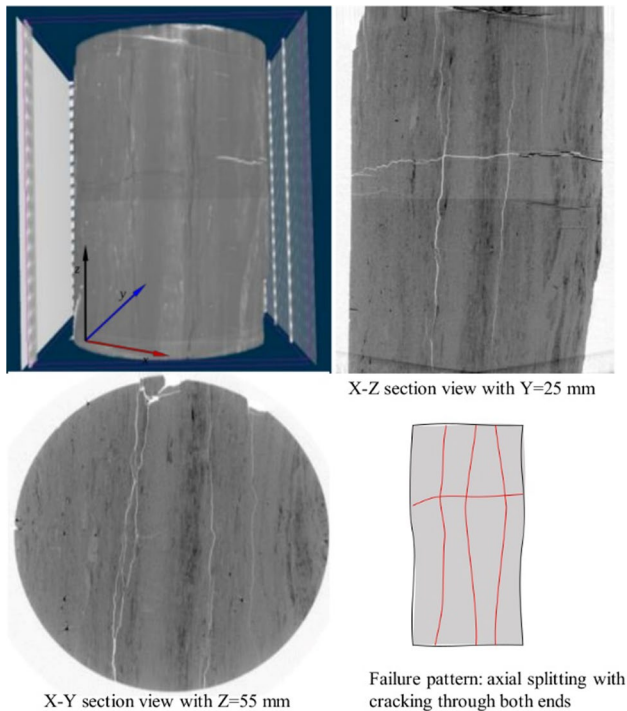
**Fig. 13** CT scan and failure pattern of sample A04
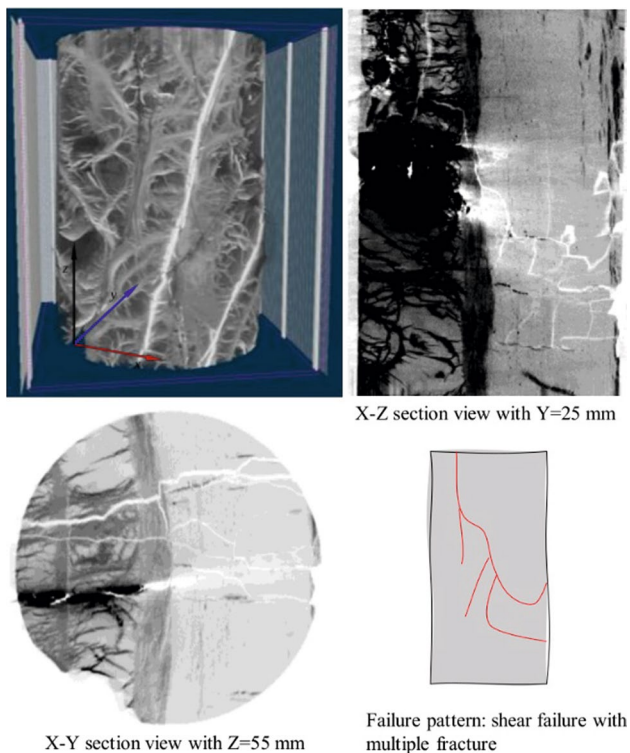
ior. The coal samples subject to cyclic fatigue load have a more fractured network with short fracture length.

These findings will be useful for understanding the coal burst under underground periodic loading conditions. However, during the research progress, the following questions have been raised, which need to be further addressed in the next stage:

(1) The unloading point was set in the stage III stable crack growth, which allows the sample to have more time to adjust the stress concentration and to develop cracks. Generally, the fracturing measures for burst control are at the beginning stage of extraction and mining works, which means that the periodic loading is not necessary started from stage III. Hence, more cyclic fatigue loading path need to be tested to comprehensively study the failure pattern of coal sample under various conditions.

(2) The previous research has indicated that loading rate and frequency have obviously influence on the mechanical behavior and failure pattern of coal/rock. In this paper, the loading rate is 0.5 mm/min, which is same with the burst propensity test standard. In the future, more loading scheme with different loading rate and frequency can be designed by referencing the complex in-site loading disturbance such as blasting, seismicity and roof movement.

(3) Only the failed sample was scanned after the test. However, due to the fragmentation of coal sample, the scan of whole failed sample is generally hard to be acquired. In the next stage tests, CT scan can be conducted several times during FLC loading stage to achieve more observation of the whole crack process.



X-Z section view with Y=25 mm

X-Y section view with Z=55 mm

Failure pattern: shear failure with multiple fracture

**Fig. 14** CT scan and failure pattern of sample B04

## Declarations

**Conflict of interest** The authors declare that they have no conflict of interest.

## References

Aldahdooh MAA, Bunnori NM (2013) Crack classification in reinforced concrete beams with varying thicknesses by mean of acoustic emission signal features. Constr Build Mater 45:282–288

Bieniawski ZT et al (1969) Failure of fractured rock. Int J Rock Mech Min Sci Geomech Abstr 6(3):323–341

Christopher M (2021) Protecting miners from coal bursts during development above historic mine workings in Harlan County, KY. Int J Min Sci Technol 31(1):111–116

Fan L, Liu SM (2019) Evaluation of permeability damage for stressed coal with cyclic loading: an experimental study. Int J Coal Geol 216:103338

Feng F et al (2022) Effects of external dynamic disturbances and structural plane on rock fracturing around deep underground cavern. Int J Coal Sci Technol 9(1):1–21. https://doi.org/10.1007/s40789-022-00487-z

Frith R et al (2020) A causation mechanism for coal bursts during roadway development based on the major horizontal stress in coal: very specific structural geology causing a localised loss of effective coal confinement and Newton's second law. Int J Min Sci Technol 30(1):39–47

Guo WY et al (2017) Effect of saturation time on the coal burst liability indexes and its application for rock burst mitigation. Geotech Geol Eng 36:589–597

Huang BX et al (2014) Experimental investigation on the basic law of hydraulic fracturing after water pressure control blasting. Rock Mech Rock Eng 47(4):1321–1334

Janeiro RP, Einstein HH (2010) Experimental study of the cracking behavior of specimens containing inclusions (under uniaxial compression). Int J Fract 164(1):83–102

Kahirdeh A et al (2016) Acoustic emission entropy as a measure of damage in materials. In: AIP conference proceedings, AIP Publishing

Kidybiński A (1981) Bursting liability indices of coal. Int J Rock Mech Min Sci Geomech Abstr 18(4):295–304

Li CW et al (2016) Study on electromagnetic radiation and mechanical characteristics of coal during an SHPB test. J Geophys Eng 13(3):391–398

Li QM et al (2019a) Acoustic emission and energy dissipation characteristics of gas-bearing coal samples under different cyclic loading paths. Nat Resour Res 29:1–16

Li TT et al (2019b) Nonlinear behavior and damage model for fractured rock under cyclic loading based on energy dissipation principle. Eng Fract Mech 206:330–341

Liu QS et al (2015) The role of flaws on crack growth in rock-like material assessed by AE technique. Int J Fract 193(2):99–115

Peng R et al (2015) Energy dissipation and release during coal failure under conventional triaxial compression. Rock Mech Rock Eng 48(2):509–526

Prem PR, Murthy AR (2017) Acoustic emission monitoring of reinforced concrete beams subjected to four-point-bending. Appl Acoust 117:28–38

Qi QX et al (2011) Study of bursting liability of coal and rock. Chin J Rock Mech Eng 30(s1):2736–2742

Ranjith PG et al (2010) The effect of $CO_2$ saturation on mechanical properties of Australian black coal using acoustic emission. Fuel 89(8):2110–2117

Singh SP (1988) Burst energy release index. Rock Mech Rock Eng 21(2):149–155

Tan LH et al (2020) Numerical study on the fracture characteristics and failure mode of hard coal under coupled static and dynamic loads. E3S Web of Conference 192:04002. https://doi.org/10.1051/e3sconf/202019204002

Tan LH et al (2021) Analytical stress solution and mechanical properties for rock mass containing a hole with complex shape. Theor Appl Fract Mech 114:103002

Wang Y et al (2020) On anisotropic fracture and energy evolution of marble subjected to triaxial fatigue cyclic-confining pressure unloading conditions. Int J Fatigue 134:105524

Wei CC et al (2022) A review of investigations on ground support requirements in coal burst-prone mines. Int J Coal Sci Technol 9(1):1–20

Xie HP (1990) Damage mechanics of rock and concrete. University of Mining and Technology Press, Xuzhou

Yang XH et al (2020) Estimation of average ejection velocity generated by rib burst under compression load. Int J Rock Mech Min Sci 128:104277

Yao QL et al (2019) Influence of moisture on crack propagation in coal and its failure modes. Eng Geol 258:105156

Zhang CG et al (2017) Assessment of energy release mechanisms contributing to coal burst. Int J Min Sci Technol 27:43–47

Zhang M et al (2020) Cyclic fatigue characteristics of strong burst-prone coal: experimental insights from energy dissipation, hysteresis and micro-seismicity. Int J Fatigue 133:105429

Zhang L et al (2021a) Acoustic emission, damage and cracking evolution of intact coal under compressive loads: experimental and discrete element modelling. Eng Fract Mech 252:107690

Zhang ZB et al (2021b) Comparative study on fracture characteristics of coal and rock samples based on acoustic emission technology. Theoret Appl Fract Mech 111:102851

Zhao HC, Kaunda RB (2018) Numerical assessment of the influences of gas pressure on coal burst liability. Energies 11(2):260

Zhao Y et al (2021) Damage evolution of coal with inclusions under triaxial compression. Rock Mech Rock Eng 54:1–18

Zheng QS et al (2020) Dynamic and damage properties of artificial jointed rock samples subjected to cyclic triaxial loading at various frequencies. Int J Rock Mech Min Sci 128:104243